

Detection of an $H\alpha$ Emission Line on a Quasar, RX J1759.4+6638, at $z = 4.3$ with AKARI

Shinki OYABU^{1,*}, Takehiko WADA¹, Youichi OHYAMA¹, Hideo MATSUHARA¹,
Toshinobu TAKAGI¹, Takao NAKAGAWA¹, Takashi ONAKA², Naofumi FUJISHIRO¹,
Daisuke ISHIHARA², Yoshifusa ITA¹, Hirokazu KATAZA¹, Woojung KIM¹,
Toshio MATSUMOTO¹, Hiroshi MURAKAMI¹, Itsuki SAKON², Toshihiko TANABÉ³,
Kazunori UEMIZU¹, Munetaka UENO⁴, Fumihiko USUI¹, Hidenori WATARAI⁵,
and Kanae HAZE¹

^{*}*e-mail:* oyabu@ir.isas.jaxa.jp

¹*Institute of Space and Astronautical Science, Japan Aerospace Exploration Agency,
3-1-1 Yoshinodai, Sagamihara, Kanagawa 229-8510, Japan*

²*Department of Astronomy, School of Science, University of Tokyo,
Bunkyo-ku, Tokyo 113-0033, Japan*

³*Institute of Astronomy, University of Tokyo,
2-21-1 Osawa, Mitaka, Tokyo, 181-0015, Japan*

⁴*Department of Earth Science and Astronomy, University of Tokyo,
3-8-1, Komaba, Meguro-ku, Tokyo 153-8902, Japan*

⁵*Office of Space Applications, Japan Aerospace Exploration Agency,
Tsukuba, Ibaraki, 305-8505, Japan*

(Received —; accepted —)

Abstract

We report the detection of an $H\alpha$ emission line in the low resolution spectrum of a quasar, RX J1759.4+6638, at a redshift of 4.3 with the InfraRed Camera (IRC) onboard the AKARI. This is the first spectroscopic detection of an $H\alpha$ emission line in a quasar beyond $z=4$. The overall spectral energy distribution (SED) of RX J1759.4+6638 in the near- and mid-infrared wavelengths agrees with a median SED of the nearby quasars and the flux ratio of $F(\text{Ly}\alpha)/F(H\alpha)$ is consistent with those of previous reports for lower-redshift quasars.

Key words: galaxies:quasars:emission lines — galaxies:quasars:individual(RX J1759.4+6638) — infrared:spectroscopy

1. Introduction

The broad emission lines of high-redshift quasars are luminous enough to study physical properties of quasars such as central black hole mass, accretion rate and metallicity of broad emission line regions in the early universe. Recent optical observations of emission lines such as C IV and N V reveal supersolar abundances in quasar broad emission line regions even at $z > 4$ (Dietrich et al. 2003). The lack of evolution of the Fe II/Mg II UV emission line ratio of quasars apparently continues out to $z=6.4$ (Barth et al. 2003; Iwamuro et al. 2004). The rest-frame optical Fe II emission as well as hydrogen Balmer emission lines in high-redshift quasars cannot be measured from the ground facilities.

These measurements can be pursued with the AKARI (Murakami et al. 2007) which has a unique capability to take near-infrared spectra in $2 - 5\mu\text{m}$ from the space as well as mid-infrared ($5\text{-}14$, $18\text{-}26\mu\text{m}$) with the InfraRed Camera (IRC; Onaka et al. 2007; Ohyama et al. 2007). Therefore one can trace the redshifted emission lines toward the high-redshift universe with the AKARI.

A quasar, RX J1759.4+6638, at a redshift of 4.320 was discovered as the most distant ROSAT X-ray selected object known at the time by Henry et al. (1994) near the North Ecliptic Pole (NEP). In this paper, we report the near-infrared spectroscopy of this quasar and the detection of an H α emission line at $z = 4.3$. Previous studies (Espey et al. 1989; Nishihara et al. 1997) performed the measurements of the H α emission line in high-redshift quasars in the near-infrared spectroscopy and the redshifts of their sample only reached $z \sim 2.4$ because the wavelength of redshifted H α emission lines is affected by strong thermal emission of a telescope. Therefore this is the first spectroscopic detection of an H α emission line in a quasar beyond $z=4$, while H α detections in photometric observations are reported by Jiang et al. (2006) for quasars at $z \sim 6$ by using the Spitzer IRAC. Our spectroscopic detection is caused by a benefit of high sensitivity spectroscopy with a cooled telescope from the space.

Through this paper, we adopt a flat cosmology with $H_0 = 71 \text{ km s}^{-1} \text{ Mpc}^{-1}$, $\Omega = 0.27$ and $\lambda = 0.73$ (Spergel et al. 2003).

2. Observation and Data Reduction

RX J1759.4+6638 was observed by the AKARI IRC on 2006 April, May, October and 2007 February. As summarized in Table 1, we made six pointed observations using the IRC spectroscopic mode AOT04. There are three observing modes: NP, NG, and NPNG modes. The NP mode uses the near-infrared prism with spectral resolving power $R \sim 19$ at $3.5\mu\text{m}$. In this mode, a target is put on the imaging area of near-infrared detector. In the NP mode, a MIR-S spectroscopic observation of a target is performed simultaneously. The NG mode uses the near-infrared grism ($R \sim 120$ at $3.6\mu\text{m}$), in which a target is put on a small aperture for a point source grism spectroscopy. The other, NPNG, is a special observing mode for a calibration

Table 1. Observing Log

Obs. ID	Obs. Date	Obs. mode*
5020047.1	2006-04-29	NPNG
5020048.1	2006-04-29	NPNG
5020049.1	2006-05-02	NPNG
5020050.1	2006-05-02	NPNG
5124035.1	2006-10-10	NG
5124044.1	2007-02-09	NP

Note.

* NP is a spectroscopy on the imaging area of detector with the near-infrared prism for resolution, $R \sim 20$, and NG is a spectroscopy on the slit of “Np” position with $R \sim 80$ of the near-infrared grism. NPNG is prepared using prism and grism in the first half observation and the second, respectively.

using the prism and the grism in the first half observation and the second, respectively. The first four observations with the NPNG mode were done for the wavelength calibration using the planetary nebula NGC 6543 in the performance verification phase. During these observations, the spectra of RX J1759.4+6638 were obtained serendipitously. The remaining observations were targeted observations for this quasar using the AKARI Director Time in order to confirm the serendipitous detections in the performance verification phase.

The data were processed through the IRC Spectroscopic toolkit (Ohyama et al. 2007) to produce calibrated data frames. The data were converted into dark-subtracted, linearity corrected and flat-field corrected frames after data that had strong cosmic rays on the target object were removed with visual investigation. Multiple frames were combined, and one-dimensional background-subtracted spectra of the target quasar were extracted from the combined data with the aperture width of 3 pixels ($4.5''$ in the NIR). The resultant spectra were scaled by a factor of 1.6 for the aperture correction. In addition to the error estimation by the IRC Spectroscopic toolkit using the sky variation near a target, we also calculated the root mean square of signal between each frames. The original error estimation was recognized to be overestimated due to the contamination of other sources and the variations of signals between each frame were used as the background error of spectra here.

The photometric calibration of the spectrum was based on AKARI IRC observations of standard stars, while the wavelength calibration was based on observations of emission line stars and planetary nebulae (Ohyama et al. 2007). At this time we estimate that the overall uncertainty in the wavelength calibration is $\sim 0.05 \mu\text{m}$ at $3.5 \mu\text{m}$.

3. Result

The series of PV phase observations (ID 5020047.1, 5020048.1, 5020049.1 and 5020050.1) detected the H α emission line only tentatively because the contamination of a faint near-infrared source affected positions of the H α emission line. The targeted NP observation (ID 5124044.1) was arranged after we checked that the dispersion direction was free from any other object using the deep N3-band image of the AKARI North Ecliptic Pole (NEP) Survey (Figure 1; Oyabu et al. 2007). The NG spectroscopy (ID 5124035.1) and all MIR-S data, which were taken simultaneously during NP observations, provided spectra with low signal-to-noise ratio only.

Figure 2 presents the resultant observed spectrum of the NP observation on the top panel with a black thick line. On the spectrum, there are two features; a bump at the wavelength of $3.47 \mu\text{m}$ and a dip on the shorter wavelength side of the bump. The bump is located at the H α emission line corresponding to $z=4.29$. For the check of their reliabilities, we divided their data in half and reduced them separately. On the top panel of Figure 2, two spectra of first and second half data are also shown in blue and red lines, respectively. Both the dip and the bump are shown in both data sets. In addition, we also checked that the response function of the NP prism did not produce these features as shown on the bottom panel of Figure 2. Thus both features, the bump and the dip, are real. The other possible explanation of the bump is the contamination of other sources. However, as mentioned above, we arranged the NP observation when the dispersion direction was free from any other objects. There is no contamination in the dispersion direction as shown in Figure 1, and therefore we conclude that the detection of the H α emission line is reliable.

To determine the wavelength center and the full width half maximum (FWHM), we fit a Gaussian function to this spectrum after smoothing the spectrum with 3 pixels (Figure 2). The detail measurements of the H α emission line are summarized in Table 1. The redshift from the H α emission line is found to be $z = 4.29 \pm 0.06$, in agreement with the previous measurements of redshifts, $z=4.320$ (Henry et al. 1994) and 4.32 (Constantin et al. 2002) by using restframe-ultraviolet emission lines from the ground-base optical spectroscopy. The H α line flux is $4.9 \pm 1.1 \times 10^{-22} \text{ W cm}^{-2}$, corresponding to the luminosity of H α emission line $L(\text{H}\alpha) = 7.5 \pm 1.7 \times 10^{36} \text{ W}$ at $z=4.3$. While the H α emission line flux is affected by two [N II] lines located at blue and red side of the H α line, their contribution of [N II] emission lines to the H α line flux is only 3 percents in the Sloan Digital Sky Survey (SDSS) composite (Vanden Berk et al. 2001) and is ignored in this paper. The FWHM of the H α emission line is found to be unresolved and $18000 \pm 4000 \text{ km s}^{-1}$ which is comparable to the instrumental resolution $\sim 20000 \text{ km s}^{-1}$ when we made the 3-pixel smoothing data. The restframe equivalent width (EW) of the H α emission line is $0.071 \pm 0.015 \mu\text{m}$ which is converted from the observed EW of $0.38 \pm 0.08 \mu\text{m}$ at $z=4.3$. However there is a dip of the continuum around $3.2 \mu\text{m}$ in Figure 2

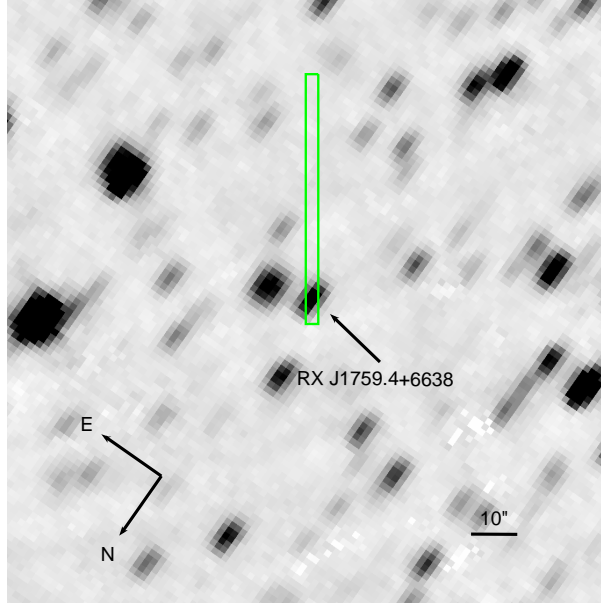


Fig. 1. The image from the NEP-Deep in the N3-band(Oyabu et al. 2007). The image is rotated as the dispersion direction is upper at 2007 Feb. 9th as the spectrum position is shown with a green box.

and the dip makes it difficult to measure the $H\alpha$ line flux and the EW accurately. This dip might be a broad absorption line feature, while there are no features of broad absorption lines in the restframe UV spectra(Henry et al. 1994; Constantin et al. 2002). Thus the reason of this dip is still uncertain.

We also measured the NIR and MIR-S photometric fluxes of this quasar with the IRC during the course of the AKARI NEP-Deep Survey (Oyabu et al. 2007)¹. The results of the NIR and MIR-S bands are summarized in Table 3. Figure 3 presents the comparison of the IRC spectrum of RX J17759.4+6638 with IRC photometric result as well as the median spectral energy distribution (SED) of low-redshift quasars (Elvis et al. 1994). Assuming that the N3-band flux includes the $H\alpha$ emission line flux and the N2- and N4-bands represent continuum level, the flux of the $H\alpha$ emission line, $F(H\alpha) = 4.0 \pm 2.6 \times 10^{-22} \text{ W cm}^{-2}$, from the photometric data agrees with the spectroscopic measurement of the $H\alpha$ emission line. The uncertainty of the line flux from the photometric data is dominated by the systematic errors of photometric calibration. The observed fluxes of emission lines and continuum level are consistent with the photometric study within their uncertainties. Comparing our measurements with the median SED of low-redshift quasars (Elvis et al. 1994), RX J1759.4+6638 has quite typical spectral energy distribution, which suggests no significant evolution in the rest-frame optical- and near-infrared wavelengths.

¹ In Oyabu et al. (2007), this quasar is called as CXOSEXSI J175928.1+663851.

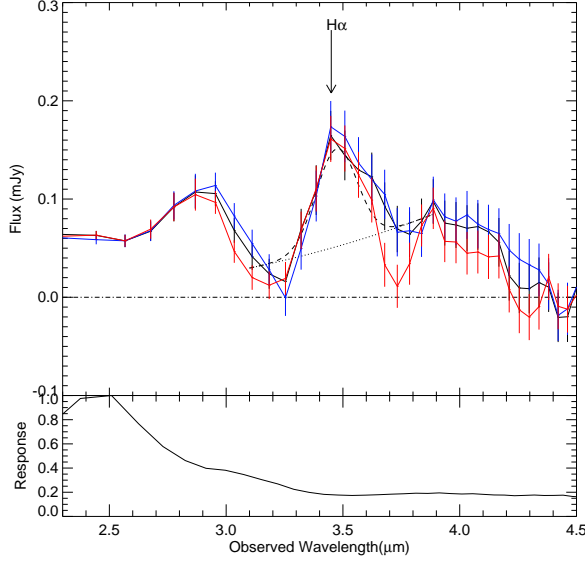


Fig. 2. The NP spectrum of RX J1759.4+6638 (black solid line; top). Blue and red lines indicate the result from first and second half of data, respectively. The vertical lines are error bars consisting of background variation, wavelength calibration, flatten calibration and flux calibration errors. The dashed and dotted lines show the fitted Gaussian and the assuming continuum, respectively. For reference, a normalized response curve of the NP as a function of wavelength (bottom).

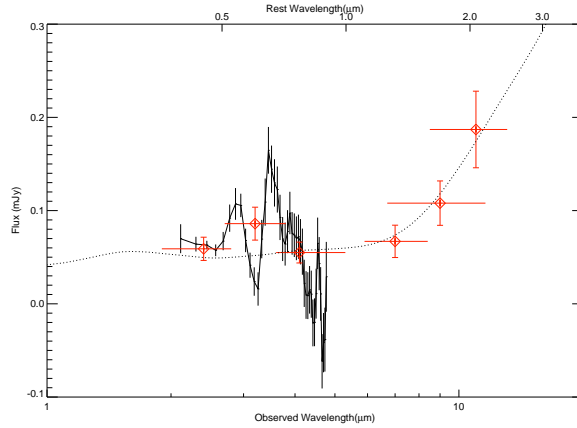


Fig. 3. Comparison of the spectrum of RX J1759.4+6638 with the photometric study. The solid line is the IRC spectrum as shown in Figure 1 with 1σ error bars, while red diamonds presents the photometric result from Oyabu et al. (2007). The red horizontal and vertical bars on each point presents the band width and the 1σ photometric error, respectively. For comparison, the median spectral energy distribution of low-redshift quasars (Elvis et al. 1994) is plotted in a dotted line after scaled at the N4-band. In Oyabu et al. (2007), this quasar is called as CXOSEXSI J175928.1+663851.

Table 2. Observed H α line measurement of RX J1759.4+6638

Line	Observed Wavelength (μm)	Redshift	Observed Flux* ($10^{-22} \text{ W cm}^{-2}$)	FWHM † (km s^{-1})	Observed EW* (μm)
H α 0.6563 μm	3.47 \pm 0.05	4.29 \pm 0.06	4.9 \pm 1.1	18000 \pm 4000 ‡	0.38 \pm 0.08

Note.

*Flux is measured by direct integration of the line flux.

† The observed full width half maximum(FWHM) of emission line.

*The observed equivalent width(EW) of emission lines.

‡ The observed FWHM is unresolved with the instrumental resolving power $\sim 20000 \text{ km s}^{-1}$ after 3 pixel smoothing at 3.5 μm .

Table 3. The AKARI/IRC photometric measurements of RX J1759.4+6638 from Oyabu et al. (2007)

Band(λ_{ref})	Flux(μJy)	Flux error(μJy)*
N2 (2.4 μm)	59	4
N3 (3.2 μm)	86	4
N4 (4.1 μm)	55	2
S7 (7.0 μm)	67	11
S9W (9.0 μm)	108	10
S11 (11.0 μm)	187	17

Note.

* Only statistical errors of the fluxes are presented. About 20 percents of the systematic errors exist during the photometric calibrations.

4. Discussion

The flux ratio of the observed H α emission line to Ly α would be useful to investigate the physical conditions in the broad-line region and the reddening to this region. Henry et al. (1994) observed the rest-frame ultraviolet spectra from ground-based telescopes, and they measured the Ly α emission line flux of $F(\text{Ly}\alpha) = 1.4 \times 10^{-21} \text{ W cm}^{-2}$ on June 1993. Constantin et al. (2002) made a new measurement of $F(\text{Ly}\alpha) = 6.4 \times 10^{-22} \text{ W cm}^{-2}$ on June 1999 with the Keck Telescope ². The Ly α line flux from Constantin et al. (2002) changed into less than half of the measurements in Henry et al. (1994) on a timescale of about 1 yr (rest frame) suggesting that this quasar is variable. We note that the X-ray observations of this quasar (Grupe et al. 2006) also reported variability. In addition, the line profile of Ly α is strongly affected by the intervening column of intergalactic neutral hydrogen (Henry et al. 1994; Constantin et al. 2002). These problems make straightforward comparisons between H α and Ly α line fluxes difficult. However assuming that the Ly α emission line flux in Constantin et al. (2002) be minimum, the lower limit, $F(\text{Ly}\alpha)/F(\text{H}\alpha) > 1.3$, is calculated. This ratio is consistent with other observational results; $F(\text{Ly}\alpha)/F(\text{H}\alpha) = 3.2$ of the SDSS composite quasar (Vanden Berk et al. 2001) and $F(\text{Ly}\alpha)/F(\text{H}\alpha) = 1.2 - 7.4$ of the low-redshift quasars at $z=0.061 - 0.555$

² Observation details are provided from A. Constantin in private communication.

(Tsuzuki et al. 2006), although the theoretical values of $F(\text{Ly}\alpha)/F(\text{H}\alpha) = 10 - 12$ from pure recombination calculation (Osterbrock & Ferland 2006) are greater than observations.

AKARI will extend the spectroscopic sample of high-redshift quasars' spectroscopy for more detailed studies of $\text{H}\alpha$ emission lines at $z > 4$. Specifically, one of the AKARI Mission Programs, "The unbiased Slit-less spectroscopic survey of galaxies (SPICY)" (Matsuhara et al. 2006), is designed and conducted to make ~ 0.5 square degree scale survey with slit-less spectroscopy with AKARI IRC wavelength and will provide a new sample of $\text{H}\alpha$ emission lines in the high-redshift universe.

5. Summary

We present the detection of an $\text{H}\alpha$ emission line on the low resolution spectrum of a quasar RX J1759.4+6638 at a redshift of 4.3 with the IRC onboard the AKARI after careful consideration of possible artifact and contamination. This is the first spectroscopic detection of an $\text{H}\alpha$ emission line in a quasar beyond $z=4$. Our spectroscopic measurement shows a good agreement with the photometric data from the AKARI NEP-Deep Survey within their uncertainties. The overall SED of RX J1759.4+6638 in the near- and mid-infrared wavelengths also agrees with a median SED of the nearby quasars. The flux ratio of $F(\text{Ly}\alpha)/F(\text{H}\alpha)$ of this quasar is consistent with those of previous report for lower-redshift quasars. These results suggest no significant evolution of the quasar's features at $z = 4.3$ in the optical- and near-infrared wavelength (rest frame).

AKARI is a JAXA project with the participation of ESA. We thank all the members of the AKARI project for their continuous help and support.

References

- Barth, A. J., Martini, P., Nelson, C. H., & Ho, L. C. 2003, *ApJL*, 594, L95
- Constantin, A., Shields, J. C., Hamann, F., Foltz, C. B., & Chaffee, F. H. 2002, *ApJ*, 565, 50
- Dietrich, M., Hamann, F., Shields, J. C., Constantin, A., Heidt, J., Jäger, K., Vestergaard, M., & Wagner, S. J. 2003, *ApJ*, 589, 722
- Elvis, M., et al. 1994, *ApJS*, 95, 1
- Espey, B. R., Carswell, R. F., Bailey, J. A., Smith, M. G., & Ward, M. J. 1989, *ApJ*, 342, 666
- Grupe, D., Mathur, S., Wilkes, B., & Osmer, P. 2006, *AJ*, 131, 55
- Henry, J. P., et al. 1994, *AJ*, 107, 1270
- Iwamuro, F., Kimura, M., Eto, S., Maihara, T., Motohara, K., Yoshii, Y., & Doi, M. 2004, *ApJ*, 614, 69
- Jiang, L., et al. 2006, *AJ*, 132, 2127
- Matsuhara et al. 2006, *PASJ*, 58, 673,

- Murakami et al. 2007, submitted to PASJ
- Nishihara, E., Yamashita, T., Yoshida, M., Watanabe, E., Okumura, S.-I., Mori, A., & Iye, M. 1997, ApJL, 488, L27
- Ohyama et al. 2007, submitted to PASJ
- Onaka et al. 2007, PASJ, in press
- Osterbrock, D.E., & Ferland, G.J., 2006, Astrophysics of Gaseous Nebulae and Active Galactic Nuclei Second Edition (University Science Books)
- Oyabu et al. 2007, submitted to PASJ
- Spergel, D. N., et al. 2003, ApJS, 148, 175
- Tsuzuki, Y., Kawara, K., Yoshii, Y., Oyabu, S., Tanabé, T., & Matsuoka, Y. 2006, ApJ, 650, 57
- Vanden Berk, D. E., et al. 2001, AJ, 122, 549